

## Gas-kinetic-based traffic model explaining observed hysteretic phase transition

Dirk Helbing and Martin Treiber

II. Institute of Theoretical Physics, University of Stuttgart, Pfaffenwaldring 57, 70550 Stuttgart, Germany

Recently, hysteretic transitions to 'synchronized' traffic with high values of both density and traffic flow were observed on German freeways [B.S.Kerner and H.Rehborn, Phys. Rev. Lett. 79, 4030 (1997)]. We propose a macroscopic traffic model based on a gas-kinetic approach that can explain this phase transition. The results suggest a general mechanism for the formation of probably the most common form of congested traffic.

05.70.Fh, 05.60.+w, 47.55.-t, 89.40.+k

To physicists, non-equilibrium phase transitions are very fascinating phenomena. Prominent examples are pattern-forming transitions in hydrodynamic systems driven far from equilibrium, like thermal convection of a fluid heated from below or transitions to a state of spatiotemporal chaos [1]. Recently, physicists got interested in the spatiotemporal, collective patterns of motion formed in social or biological systems of so-called 'motorized' or 'self-driven' particles [2]. A particularly strong physical activity has developed in the rapidly growing field of traffic dynamics [3-16], not only because of the large potential for industrial applications.

On a macroscopic scale, many aspects of traffic flow are similar to those of aggregated physical systems. In particular, if one abstracts from the motion of the single vehicles, traffic can be modelled as a continuum compressible fluid [4,5] (see Ref. [6] for an overview). Existing macroscopic traffic models have been able to explain various empirically observed properties of traffic dynamics, including the transition of slightly disturbed traffic to traffic jams ('local cluster effect') [7].

Recently, Kerner and Rehborn presented experimental data indicating a first-order transition to 'synchronized' traffic (ST) [8]. Traffic data from several freeways in Germany [8,9] and the Netherlands [6,10] indicate that ST is the most common form of congested traffic. ST typically occurs at on-ramps when vehicles are added to already busy 'freeways' and has the following properties: (i) The dynamics of the average velocities on all lanes is highly correlated ('synchronized'). (ii) ST is characterized by a low average velocity, but, in contrast to traffic jams, the associated traffic flow is rather high. (iii) The transition to ST is usually caused by a localized and short perturbation of traffic flow that starts downstream of the on-ramp and propagates upstream with a velocity of about 10 km/h. (iv) As soon as the perturbation passes the on-ramp, it triggers ST which spreads upstream in the course of time. (v) Downstream, ST eventually relaxes to free traffic. (vi) ST often persists over several hours. (vii) The transition from ST to free traffic occurs at a lower density and higher average velocity than the inverse transition (hysteresis effect).

Property (i) is related to lane-changing and requires a multi-lane model for its description, e.g. [11]. In order

to explain the other characteristic properties of ST, we will propose a macroscopic, effective one-lane model that was derived from a gas-kinetic level of description and treats all lanes in an overall manner. The model is also in agreement with other empirical findings [9,12] like the existence of metastable states, the typical propagation velocity of upstream jam fronts (between 10 and 20 kilometers per hour), and the characteristic outflow  $Q_{out}$  from traffic jams of 1600 up to 2100 vehicles per hour and lane (depending on the road and weather conditions, but not on the initial conditions or the surrounding traffic density) [13].

Our model is based on a kinetic equation for the phase-space density  $\tilde{n}(x;v;t)$ , which corresponds to the spatial vehicle density  $\rho(x;t)$  times the distribution  $P(v;x;t)$  of vehicle velocities  $v$  at position  $x$  and time  $t$  [5]. (For an introduction to gas-kinetic traffic models see Ref. [14].) The kinetic equation has some similarities to the gas-kinetic Boltzmann equation for one-dimensional dense gases with the vehicles playing the role of molecules. However, there are also some features specific to traffic. Drivers want to accelerate to their respective desired velocities giving rise to a relaxation term that violates conservation of momentum and kinetic energy. Moreover, when approaching a slower car that cannot be immediately overtaken, one has to decelerate while the car in front remains unaffected. This leads to an anisotropic interaction. Finally, the reaction of the drivers depends on the traffic situation ahead of them, making the interaction non-local.

The model equations for the lane-averaged vehicle density  $\rho(x;t) = \int_R dv \tilde{n}(x;v;t)$  and the average velocity  $V(x;t) = \frac{1}{\rho} \int_R dv v \tilde{n}(x;v;t)$  are

$$\frac{\partial}{\partial t} + \frac{\partial(V)}{\partial x} = \frac{Q_{mp}}{nL}; \quad (1)$$

$$\frac{\partial}{\partial t} + V \frac{\partial}{\partial x} = \frac{1}{\rho} \frac{\partial(\rho V)}{\partial x} + \frac{V_0 - V}{\tau} + \frac{V_0 A(\rho) (A_{max} TV)^2}{A(\rho_{max}) (1 - \frac{A(\rho)}{A_{max}})^2} B(V); \quad (2)$$

where we use the notation  $f_a(x;t) = f(x_a;t)$  with  $f = \rho, V, g$  and an advanced 'interaction point'  $x_a$  specified

later. Without on- or off-ramps, the density equation (1) is just a one-dimensional continuity equation reflecting the conservation of the number of vehicles. Thus, the temporal change  $\partial Q / \partial t$  of the vehicle density is just given by the negative gradient  $-\partial Q / \partial x$  of the lane-averaged traffic flow  $Q = V \rho$ . Along on-ramps (or off-ramps), the source term  $Q_{mp} = (nL)$  is given by the actually observed inflow  $Q_{mp} > 0$  from (or outflow  $Q_{mp} < 0$  to) the ramp, divided by the merging length  $L$  and by the number  $n$  of lanes. The inflow has an upper limit that depends on the downstream flow on the main road [15].

The velocity equation (2) contains the velocity variance  $\langle x; t \rangle = \frac{1}{V} \int_0^V [V(x; t) - V(x; t)]^2 dx; t$ . Instead of deriving a dynamic equation for  $\langle x; t \rangle$  from the kinetic equations, we use the constitutive relation  $A(\rho) = A_0 + A_1 \rho + \tanh \left( \frac{\rho - \rho_{max}}{\rho_{max}} \right) \frac{c}{\rho_{max}}$ ; (3)

where  $A_0 = 0.008$ ,  $A_1 = 0.015$ ,  $c = 0.28 v_{max}$ , and  $\rho_{max} = 0.1 \text{ km}^{-1}$  [13]. These coefficients can be obtained from single-vehicle data. Unfortunately, no such data were available for the motorway considered in [8], but similar values were obtained for another motorway [16].

The first term on the rhs of Eq. (2) is the gradient of the 'traffic pressure'. It describes the kinematic dispersion of the macroscopic velocity in inhomogeneous traffic as a consequence of the finite velocity variance. For example, the macroscopic velocity in front of a small vehicle cluster will increase even if no individual vehicle accelerates, because the faster cars will leave the cluster behind. The second term denotes the acceleration towards the (traffic-independent) average desired velocity  $V_0$  of the drivers with a relaxation time  $\tau = 2$  [10 s, 50 s]. Individual variations of the desired velocity are accounted for by a finite velocity variance. The third term of the rhs of Eq. (2) models braking in response to the traffic situation at the advanced 'interaction point'  $x_a = x + (l = \rho_{max} + TV)$ . In dense traffic, where most drivers maintain the safety distance  $TV$ , this point is about vehicle positions in front of the actual vehicle position  $x$ . The average safe time headway  $T$  is of the order of one second. For the 'anticipation factor', we assume values between one and two. The braking deceleration increases Coulomb-like with decreasing gap ( $l = a = l_{max}$ ) to the car in front ( $l = a$  being the average distance between successive vehicle positions,  $l = \rho_{max}$  the average vehicle length, and  $\rho_{max}$  the maximum density). In homogeneous dense traffic, the acceleration and braking terms compensate for each other at about the safe distance. In general, the deceleration tendency depends also on the velocity difference to the traffic at the interaction point. A gas-kinetic derivation leads to the 'Boltzmann factor' [13]

$$B(v) = 2 \frac{e^{-\frac{v^2}{2}}}{v} + (1 + \frac{v}{V_0}) \frac{Z}{1} \frac{e^{-\frac{v^2}{2}}}{2} dy; (4)$$

where  $v = (V - V_a) = \frac{p}{a} + \frac{p}{a}$  is the dimensionless velocity difference between the actual location  $x$  and the interaction point  $x_a$ . In homogeneous traffic, we have  $B(0) = 1$ . If the preceding cars are much slower (i.e.  $v \rightarrow 0$ ), it follows  $B(v) = 2 \frac{v}{V_0}$ . In the opposite case (i.e.  $v \rightarrow 0$ ), we have  $B(v) \rightarrow 0$ . That is, since the distance is increasing, then, the vehicle will not brake, even if its headway is smaller than the safe distance.

In contrast to previous approaches, the above macroscopic traffic model explicitly contains an anisotropic, non-local interaction term  $B(v)$ . This is not only essential for a realistic treatment of situations with large gradients of  $\langle x; t \rangle$  or  $V(x; t)$ , but also for an efficient and robust numerical integration. Moreover, the prefactor of  $B$  has now been obtained from the plausible assumption that, at high densities, the time headway between successive vehicles is  $T$ . Finally, all model parameters are meaningful, measurable, and have the correct order of magnitude.

Our simulations have been carried out with an explicit finite-difference integration scheme and the following parameter values:  $V_0 = 128 \text{ km/h}$ ,  $\rho_{max} = 160 \text{ vehicles/km}$ ,  $T = 1.6 \text{ s}$ ,  $\tau = 31 \text{ s}$ , and  $\alpha = 1.0$ . The response of equilibrium traffic to localized disturbances is similar to the Kerner-Konhäuser model [7]. For densities  $\rho < \rho_{c1}$  and  $\rho > \rho_{c4}$ , homogeneous traffic is stable, and for a range  $\rho_{c2} < \rho < \rho_{c3}$  of intermediate densities, it is linearly unstable, giving rise to cascades of traffic jams ('stop-and-go traffic'). For the two density regimes  $\rho_{c1} < \rho < \rho_{c2}$  and  $\rho_{c3} < \rho < \rho_{c4}$  between the stable and the linearly unstable regions, it is metastable, i.e., it behaves nonlinearly unstable with respect to perturbations exceeding a certain critical amplitude, but otherwise stable. For the self-organized density  $\rho_{jam}$  inside traffic jams we find a typical value  $\rho_{jam} > \rho_{c4}$  [13].

Now, we will discuss synchronized flow. Figure 1 shows the simulation of freeway traffic near an on-ramp during a 'rush-hour', where we assumed that the flow downstream of the on-ramp almost reaches the maximum equilibrium flow ('capacity limit')  $Q_{max}$ . The upstream boundary condition at position  $x_0 = 6 \text{ km}$  was specified in accordance with the equilibrium flow-density relation for free traffic (dotted lines in Fig. 3, before the maximum of the curve) with flows according to Fig. 1(c). We started with a high main flow that is monotonically decreasing in the course of time. At  $x = 0 \text{ km}$ , an on-ramp with merging length  $L = 300 \text{ m}$  injects an additional time-dependent inflow  $Q_{mp}$  into the freeway. This on-ramp flow was assumed to have a short and tiny peak at  $t = 10 \text{ min}$  in Fig. 1(c). As a result, a wave of denser traffic propagated downstream, thereby gaining a larger amplitude, and eventually propagated upstream again with about

11 km/h. Once the perturbation reached the ramp, dense traffic (of about 48 vehicles/km) with relatively high flows (1600 vehicles/h) corresponding to  $V = 33 \text{ km/h}$  built up in the upstream direction. Although the

flow from the main road was gradually decreased for  $t > 30$  min, it took more than 100 additional minutes, until the region of congested traffic vanished.

All these features agree with the experimental observations of ST described in Ref. [8]. There, a peak on the on-ramp flow was observed at about 7:15 am. The transition to ST was first detected at 7:16 am as a short dip of the velocity 700 m downstream from the on-ramp (detector D3 in [8]). At about 7:22 am, the front reached a detector (D2) 200 m upstream of the ramp (corresponding to a mean propagation speed of 11 km/h), and propagated slower to the next detector D1 (700 m upstream). While the perturbation at detector D3 lasted only a few minutes, it was followed by nearly 2 hours of congested traffic ( $V = 30$  km/h,  $Q = 1500$  vehicles/h) at the detectors D2 and D1.

It turned out that, apart from fluctuations, the simulated velocities and flows obtained at the detector positions  $x = 0.7$  km (D1),  $x = 0.2$  km (D2),  $x = 0.7$  km (D3), and  $x = 1.5$  km (D4) (cf. Fig. 2) are in almost quantitative agreement with all features of ST as displayed in Figs. 2(c), 2(b), 2(a), and 2(d) of Ref. [8]. In particular, the model reproduces the drop of the velocity to about 30 km/h for up to two hours, while the flow is reduced by only 20%. Moreover, after the transition to free flow, the velocity is higher and the flow is lower than immediately before the transition to synchronized flow, both in the measurements and the simulation. Finally, in Fig. 3 we depict the relaxation to free traffic downstream of the ramp by flow-density diagrams [see also Fig. 1(b)]. The results agree well with the empirical traffic data presented in Fig. 3(c) of Ref. [8].

Our results suggest the following interpretation of the phase transition to ST. Initially, the homogeneous flow  $Q_{\text{main}}$  upstream of an on-ramp is stable, while the higher downstream flow  $Q_{\text{down}} = Q_{\text{main}} + Q_{\text{mp}} = n$  is metastable ( $n = \text{number of lanes}$ ). A perturbation of the ramp flow  $Q_{\text{mp}}$  triggers a stop-and-go wave, which travels downstream as long as it is small and upstream as it becomes larger, as is known from 'localized clusters' [7]. Now, assume the downstream front of the cluster would pass the on-ramp. Then, since  $Q_{\text{main}}$  [Fig. 1(c)] is lower than the characteristic outflow  $Q_{\text{out}}$  from a jam (being of the order of 2000 vehicles/km), the cluster would eventually vanish. However, during its lifetime, the cluster would continue to emit the flow  $Q_{\text{out}}$ , leading downstream of the ramp to a flow  $Q_{\text{out}} + Q_{\text{mp}} = n > Q_{\text{max}}$ . As a consequence, as soon as the perturbation reaches the on-ramp, it induces congested traffic with a standing downstream front just at the end of the ramp. With an observed outflow  $\tilde{Q}_{\text{out}} < Q_{\text{out}}$  from ST [17], the average flow upstream is given by

$$Q_{\text{sync}} = \tilde{Q}_{\text{out}} - Q_{\text{mp}} = n : \quad (5)$$

Now, consider the density  $\rho_{\text{sync}}$  defined by  $Q_{\text{sync}} = Q_e(\rho_{\text{sync}})$  in the congested part of the equilibrium flow-

density relation  $Q_e(\rho)$  (dotted lines in Fig. 3, behind the maximum of the curves). If homogeneous traffic is (meta-)stable at  $\rho_{\text{sync}}$ , the on-ramp induces ST, otherwise it induces dynamically changing states. The restriction  $Q_{\text{mp}} - \tilde{Q}_{\text{out}} = 2$  [15] (corresponding to every second vehicle on the right freeway lane stemming from the on-ramp) implies  $Q_{\text{sync}} = (1 - \frac{1}{2n})\tilde{Q}_{\text{out}}$  and  $\rho_{\text{sync}} < \rho_{\text{jam}}$ , so that synchronized flow is significantly higher than the flow inside traffic jams.

We have proposed a macroscopic traffic model based on a gas-kinetic level of description that allows to describe the empirically observed features of traffic flows. This Letter focussed on the simulation and interpretation of ST, which is probably the most common form of congested traffic. We have triggered ST by a small peak in the inflow from an on-ramp, when the downstream flow was close to freeway capacity. Synchronized traffic eventually resolved in downstream direction, but spread in upstream direction. It persisted for more than one hour, although the main flow was steadily reduced. We also performed simulations without peaks, leaving everything else unchanged. In these cases, we obtained free traffic flow. This confirms that the proposed model can describe the hysteretic and bistable properties of real traffic. Our interpretation of ST underlines the crucial role of the characteristic outflow  $Q_{\text{out}}$  from congested traffic for traffic dynamics. The simple criterion  $Q_{\text{out}} + Q_{\text{mp}} = n > Q_{\text{max}}$  for the formation of ST can be useful for determining bottlenecks of the existing road infrastructure as well as for planning efficient freeway networks.

The authors want to thank for financial support by the BM BF (research project SANDY, grant No. 13N 7092) and by the DFG (Heisenberg scholarship He 2789/1-1).

- 
- [1] M. C. Cross and P. C. Hohenberg, Rev. Mod. Phys. 65, 851 (1993); M. Dennin, M. Treiber, and L. Kramer, Phys. Rev. Lett. 76, 319 (1996).
  - [2] T. Vicsek et al., Phys. Rev. Lett. 75, 1226 (1995); H. J. Bussemaker et al., Phys. Rev. Lett. 78, 5018 (1997); E. Ben-Jacob et al., Nature 368, 46 (1994).
  - [3] R. Herman et al., Science 179, 918 (1973); R. Herman and I. Prigogine, Science 204, 148 (1979); W. Leutzbach, Introduction to the Theory of Traffic Flow (Springer, Berlin, 1988); D. E. Wolf et al. (eds.) Traffic and Granular Flow (World Scientific, Singapore, 1996); L. F. Henderson, Nature 229, 381 (1971); D. Helbing et al., Nature 388, 47 (1997).
  - [4] M. J. Lighthill and G. B. Whitham, Proc. Roy. Soc. A 229, 317 (1955); B. S. Kerner and P. Konhäuser, Phys. Rev. E 50, 54 (1994); D. Helbing, Phys. Rev. E 51, 3164 (1995).

- [5] D. Helbing, Physica A 233, 253 (1996).  
[6] D. Helbing, Verkehrsdynamik (Springer, Berlin, 1997).  
[7] B. S. Kerner, P. Konhäuser, and M. Schilke, Phys. Rev. E 51, 6243 (1995).  
[8] B. S. Kerner and H. Rehborn, Phys. Rev. Lett. 79, 4030 (1997).  
[9] B. S. Kerner and H. Rehborn, Phys. Rev. E 53, R4275 (1996).  
[10] D. Helbing, Phys. Rev. E 55, R25 (1997).  
[11] D. Helbing, Physica A 242, 175 (1997).  
[12] B. S. Kerner and H. Rehborn, Phys. Rev. E 53, R1297 (1996).  
[13] M. Treiber, A. Hennecke, and D. Helbing, APS preprint e-sub1998jun24\_008 (1998).  
[14] I. Prigogine and R. Hemmen, Kinetic Theory of Vehicular Traffic (Elsevier, New York, 1971); D. Helbing, Phys. Rev. E 53, 2366 (1996); P. Nelson, Transp. Theor. Stat. Phys. 24, 383 (1995); C. Wagner et al., Phys. Rev. E 54, 5073 (1996); T. Nagatani, Physica A 237, 67 (1997).  
[15] C. F. Daganzo, unpublished (1998).  
[16] D. Helbing, Phys. Rev. E 55, 3735 (1997).  
[17] Simulations show that  $\bar{Q}_{out}$  is a function of the merging length  $L$  with  $\lim_{L \rightarrow 1} \bar{Q}_{out}(L) = Q_{out}$ .  $\bar{Q}_{out}(L) < Q_{out}$  is a capacity drop effect due to disturbances by finite on-ramps. Here we obtained  $\bar{Q}_{out} = 1877$  vehicles/h, and  $Q_{out} = 2000$  vehicles/h.

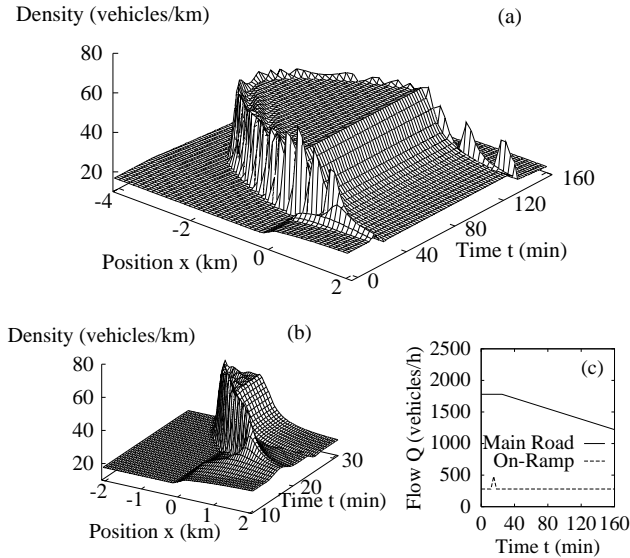


FIG. 1. Spatio-temporal evolution of the lane-averaged density after a small peak of inflow from the on-ramp. The on-ramp merges with the main road at  $x = 0$  km with a merging length of 300 m. Trajectories from left to right. In (a), the parabolically shaped region of high density corresponds to ST. Plot (b) shows the formation of this state in more detail. The time-dependent inflows  $Q_{main}$  at the upstream boundary and  $Q_{on-ramp}$  at the on-ramp are displayed in (c).

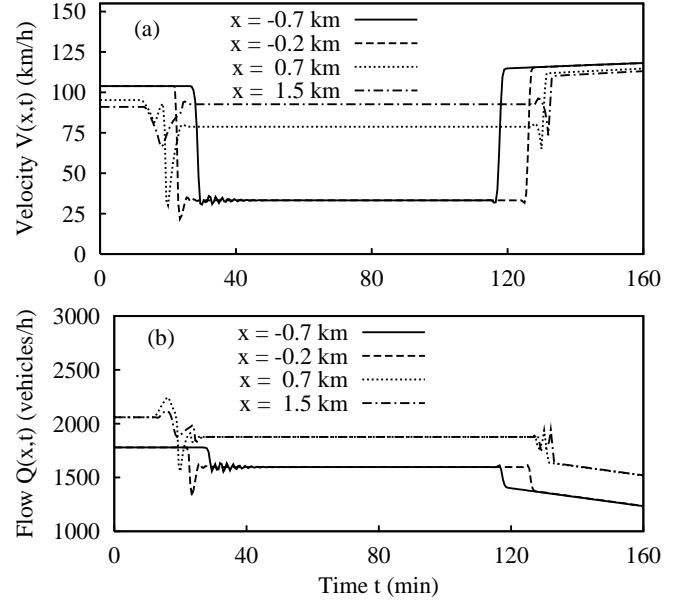


FIG. 2. Temporal evolution of (a) the average velocity and (b) the traffic flow per lane at four cross sections of the freeway near the on-ramp. In front of the on-ramp ( $x < 0$ ), ST exists for a certain time interval. Downstream ( $x > 0$ ), the traffic situation recovers towards a freely flowing state. The simulated overshooting at the beginning of the breakdown of average velocity is in agreement with empirical observations (cf. Fig. 1 (b) in Ref. [8]).

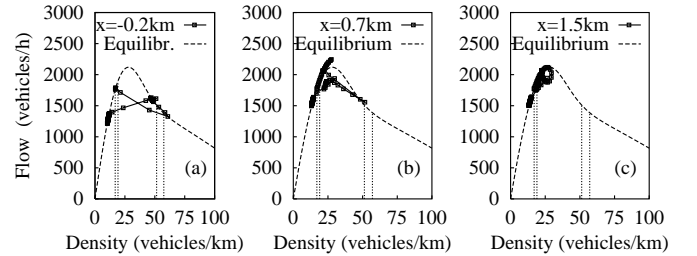


FIG. 3. Traffic dynamics in the flow-density plane (a) 0.2 km upstream of the on-ramp and (b), (c) at two downstream cross sections. The solid lines with the symbols (2) correspond to the simulation results of Fig. 1. All the trajectories start at  $\rho = 17$  vehicles/km and  $Q = 1770$  vehicles/h. The dashed line represents the equilibrium relation  $Q_e(\rho)$  of the model. The vertical dotted lines indicate the stability limits  $\rho_{c1}$ ,  $\rho_{c2}$ ,  $\rho_{c3}$ , and  $\rho_{c4}$  (determined numerically).